Article,

Studying anti-virulence activity of meta-bromo-thiolactone against *Staphylococcus aureus* and MRSA phenotypes

Rihaf Alfaraj[1*], Esra K. Eltayb[1], Bashayer M. AlFayez[1], Amjad S. Abohamad[1], Eram Eltaher[1], Naifa A. Alenazi[1], Sandra Hababah[1], Hamad Alkahtani[2], Thamer A Almangour[3], Fulwah Y. Alqahtani[1], Fadilah S. Aleanizy[1]

1. Department of Pharmaceutics, College of Pharmacy, King Saud University, Riyadh 11495, Saudi Arabia
2. Department of Pharmaceutical Chemistry, College of Pharmacy, King Saud University, Riyadh 45142, Saudi Arabia
3. Department of Clinical Pharmacy, College of Pharmacy, King Saud University, P.O. Box 22452 Riyadh 11495, Saudi Arabia

* Correspondence: Rihaf Alfaraj, PhD, email; ralfaraj@ksu.edu.sa

Abstract: Quorum-sensing inhibitors have recently garnered great interest, as they reduce bacterial virulence, lower the probability of resistance, and refining infections. In this work, meta-bromo-thiolactone (mBTL), a potent quorum and virulence inhibitor of Staphylococcus aureus and methicillin-resistant S. aureus (MRSA), was formulated in chitosan nanoparticles (ChNPs) using the ionic gelation method. mBTL-loaded-ChNPs were characterized for particle size, polydispersity index, zeta potential, morphology, and drug release profile. Synthesized mBTL-loaded-CNPs showed homogenized nanosize particles ranging from 158±1.3 to 284±5.6 nm with spherical particles that exhibited a sustainable release profile over 48 h at 37°C. These findings revealed the successful preparation of mBTL-loaded-ChNPs. Confocal laser scanning microscopy showed a significant reduction in the number of viable cells, indicating the effectiveness of mBTL as an antibacterial agent. The formed biofilms were clearly distinguished in the scanning electron microscopy images. Bacterial cells in the control group were enclosed in thick biofilms. By contrast, there was a considerable reduction in biofilm production when mBTL was present, and the bacterial cells seemed less ordered and more scattered with no detectable biofilm. In conclusion, mBTL-loaded-ChNPs are a potential alternative treatment to overcome antimicrobial resistance and treat MRSA infection.

Keywords: *Staphylococcus aureus*, MRSA, mBTL, mBTL-ChNPs, antibiotic resistance, quorum sensing, virulence, biofilm.

1. Introduction

MRSA refers to methicillin-resistant Staphylococcus aureus, a bacterium resistant to many available antibiotics, including β-lactam. MRSA is the predominant pathogen contributing to antimicrobial resistance (AMR) in both community and health care settings. Studies have shown that 33% of people carry S. aureus in their nose without harm, and two out of every hundred are MRSA carriers [1]. The consequences of the MRSA infection continue to upsurge, because of elevation in transmission rates, intense colonization, and rapid bacterial activation of virulence factors that increase the infection's pathogenicity. The population expanding of the bacteria is subjected to a chemical signaling mechanism named as quorum sensing (QS), which allow a cell-to-cell communication. In S. aureus, quorum-sensing accessory gene regulator (agr) system controls the virulence factors production. Therefore, at high cell density, agr is activated leading to the secretion of an auto-inducing peptide (AIP), that is detected by the trans-membrane receptors leading to activation of the bacterial virulence factors that cause the infection. S. aureus pathogenicity is highly dependent on the virulence factors such as toxins (Hemolysins), immune-evasive surface factors (capsule and protein A),

Preprints (www.preprints.org) | NOT PEER-REVIEWED | Posted: 8 June 2023 doi:10.20944/preprints202306.0628.v1

and biofilm formation [3]. S. aureus has two QS systems produced by agr locus; RNAII that originates from the P2 promoter, and RNAIII that originates from the P3 promoter. The RNAIII segment of agr is generated from four genes agr A, B, C and D, which encode all the main components of the QS system. The trans-membrane protein agr B is involved in AIP signal secretion, modification and agr D processing. Whereas, the agr A encodes the cytosolic response regulator (RR), and the agr C encodes membrane-bound histidine kinase (HK), however, they both form the two components regulatory system (AgrAC TCS) [4]. A Previous study has reported that synthetic molecules of meta-bromo-thiolactone (mBTL) have inhibited virulent bacterial QS, and provided the uppermost activity for QS system inhibition [5]. Using mBTL molecules, quorum sensing system can be regulated, thus it can be a potential alternative for antibiotic therapy and an approach to reduce the MDR issue. The therapeutic index of pharmacological activity of agents can be increased due to the prolonged release of drugs via polymeric nanoparticles [6]. Chitosan refers to a class of polymers derived from chitin; a natural polysaccharide comprised of-(1,4)-linked N-acetyl glucosamine units. Fungi and the exoskeletons of crustaceans and insects are the most prevalent sources of chitin [7]. Chitosan-based nanoparticles can be utilized to deliver active components, such as pharmaceuticals or natural products, via a variety of modes of administration. Chitosan nanoparticles combine the unique characteristics of the polymer with tunable size and the capacity to modify the surface to meet specific demands, making them a very promising and diverse solution for overcoming the bioavailability and stability difficulties that affect most active ingredients [7]. The aim of this work is to formulate mBTL in chitosan nanoparticles, and test their effect on S. aureus, MRSA and QS various mutants mostly biofilm effect.

2. Results

2.1. Nanoparticles Characterization

In this study, average particle size, polydispersity index (PDI), and zeta potential were investigated. The particles size was 158.5 ±1.3 nm and 283.9±13.55 nm for blank ChNPs and mBTL-ChNPs respectively, which was less than 500 nm and considered in the nanosized range. However, PDI values were of 0.3 and below that indicated the formation of homogenous preparations. In addition, the zeta potential of chitosan nanoparticles was positively charged which indicated good physical stability of the nano-preparations as shown in Table 2. The morphological visualization of the ChNPs were carried out using TEM as shown in Figure 1.

Table 2. Nanoparticles characteristics all data are presented as mean ±SD.

	Blank ChNPs	mBTL-ChNPs
Particle size	158.5 ±1.3	283.9±13.55
PDI	0.327 ± 0.016	0.253±0.018
Zeta potential	33.8 ± 0.361	19.6±1.25

Preprints (www.preprints.org) | NOT PEER-REVIEWED | Posted: 8 June 2023 doi:10.20944/preprints202306.0628.v1

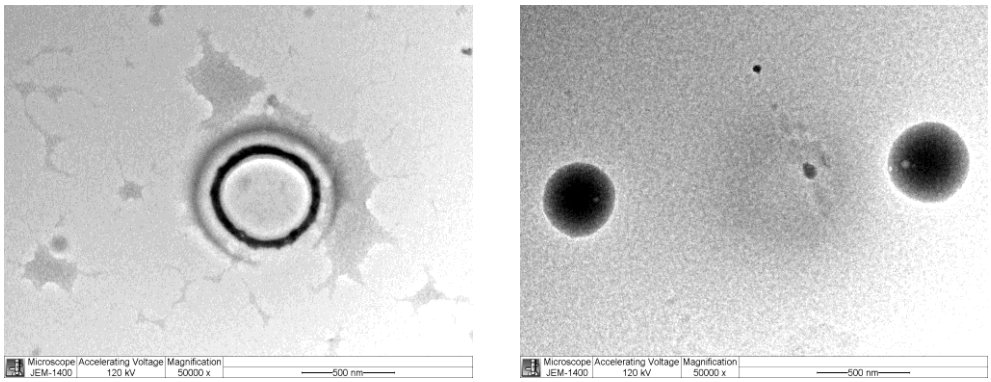

Figure 1. TEM images: (a) blank ChNPs and; (b) mBTL-loaded ChNPs. (a) (b)

2.2. Encapsulation efficacy of mBTL-ChNPs

Encapsulation of mBTL n ChNPs was determined by assessing the percentage of encapsulation efficiency (EE%) and validated based on calibration curve of mBTL. The percentage of fresh mBTL incapsulated inside ChNPs was 70.358 %.

2.3. In vitro Drug Release

In-vitro release of mBTL in 30 ml of the phosphate buffer at pH 7.4 over 24, and 48 hours as a time of function using cellulose dialysis tube sealed at both ends. The release profile of mBTL was obtained by plotting the cumulative percentage release of the mBTL versus time as shown in Figure 2.

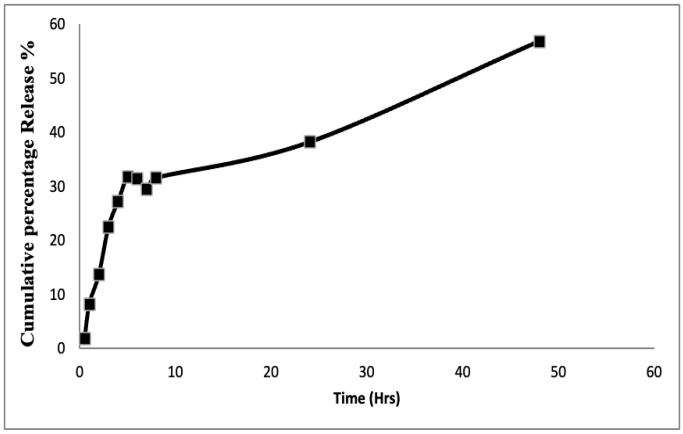

Figure 2. *In-vitro* release profile of free mBTL.

2.4. Growth pattern of S. aureus and other mutants in the presence and absence of mBTL and mBTL-ChNPs

The effect of mBTL and mBTL-ChNPs and plain ChNPs were investigated using a wild type *S. aureus*, MRSA, and different staphylococcus QS mutants; NE1532 (AgrA), NE95 (AgrB) and NE873 (AgrC). Oxacillin was used as a positive control. The selected concentrations of mBTL were 2 mg/ml, 1 mg/ml and 0.5 mg/ml (Figure 3). The growth of all strains was evaluated against plain ChNPs to antimicrobial effect and the results showed that all strains exhibited similar growth pattern as the untreated strains and the used ChNPs is cytocompatible and has no bactericidal effect.

Preprints (www.preprints.org) | NOT PEER-REVIEWED | Posted: 8 June 2023 doi:10.20944/preprints202306.0628.v1

In the presence of mBTL-ChNPs, the growth of all strains was reduced significantly ($p< 0.05$) displaying 60.83%, 98.76%, 100%,100% and 100% reduction in growth of the wild type of *S. aureus*, MRSA and the different staphylococcus QS mutants, NE1532 (AgrA), NE95 (AgrB), NE873 (AgrC) respectively. mBTL alone have showed a reduction in the growth of all strains, however, when loaded in ChNPs the uptake increased and it showed an enhanced killing effect.

Concentrations ranging from 2 mg/mL to 0.125 mg/mL of both free mBTL and mBTL-ChNPs were tested for antimicrobial activity in the present study. The MIC50 was determined using the broth dilution method, which was used to screen for antimicrobial effect. Bacterial growth analysis demonstrated a dose-dependent effect on mBTL, where 2 and 1 mg/ml showed 100% killing effect, however, there was a reduction in bacterial growth, the MIC_{50} was 0.5mg/ml for mBTL-ChNPs concentration was chosen for further analysis of virulence inhibitory effect.

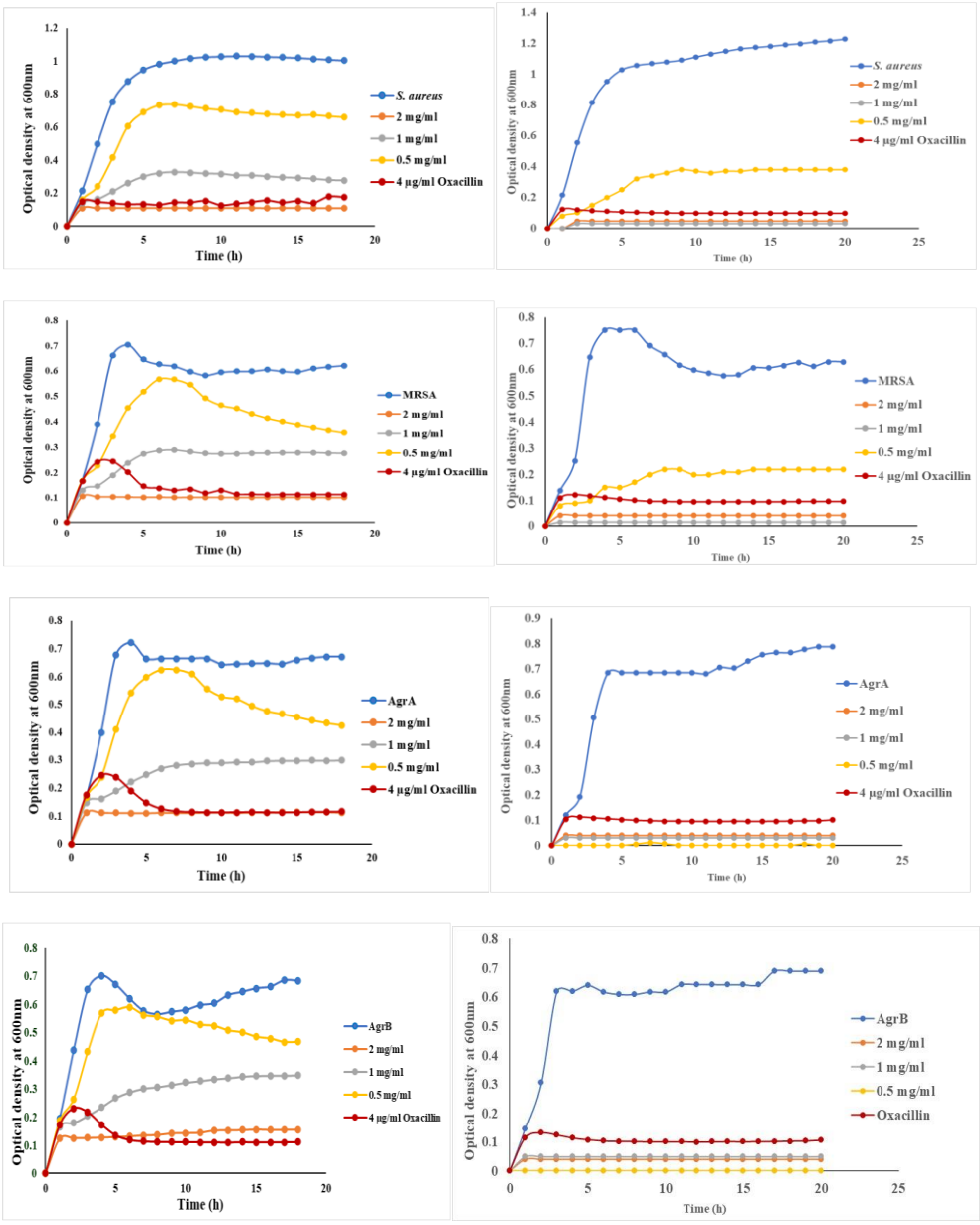

Preprints (www.preprints.org) | NOT PEER-REVIEWED | Posted: 8 June 2023 doi:10.20944/preprints202306.0628.v1

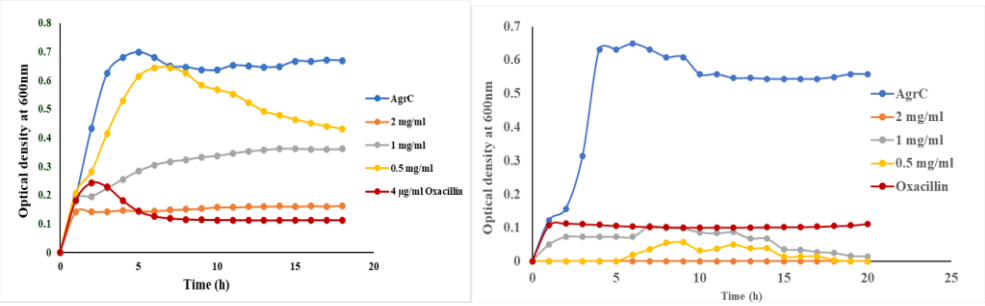

(a) (b)

Figure 3. The effect of free mBTL (Lane (a)) The effect of mBTL-loaded-ChNPs (Lane (b)) investigated using wild type *S. aureus*, MRSA, and different staphylococcus QS mutants; NE1532 (AgrA), NE95 (AgrB), NE873 (AgrC). All experiment performed three times in triplicate.

2.5. Biofilm inhibitory of S. aureus and other mutant in response to the free mBTL.

The anti-virulence effect of mBTL-ChNPs against biofilm was investigated using *S. aureus*, MRSA, and different *Staphylococcus* QS mutants, NE1532 (AgrA), NE95 (AgrB) and NE873 (AgrC). The inhibition of biofilm was showed in (figure-3). Results showed around 51.7% and 50% of biofilm reduction for *S. aureus*, MRSA, whereas around 68% and 63.6% for mutants NE1532 (AgrA), NE95 (AgrB)and showed significant reduction of biofilm ($p< 0.05$) around 97.3% for mutant NE873 (AgrC) as shown in figure 4.

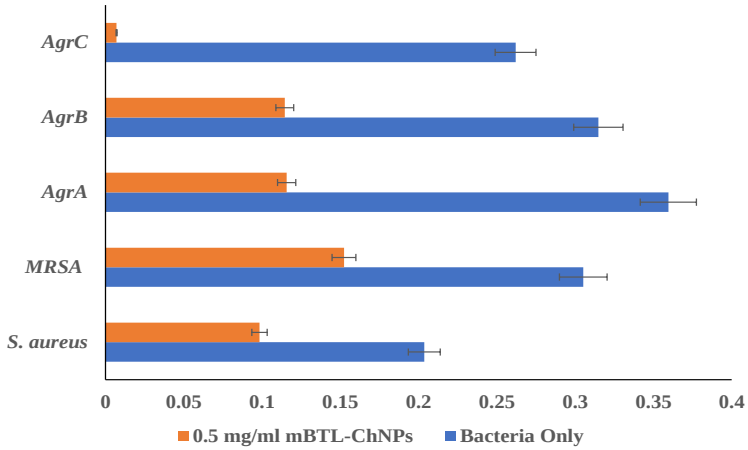

Figure 4. Anti-virulence effect of Loaded-mBTL against Biofilm using wild type Staphylococcus aureus, MRSA and QS mutants, NE1532 (AgrA), NE95 (AgrB) and NE873 (AgrC).

2.6. Assessment of bacterial viability within formed bacterial biofilm after exposure to prepared nanoparticles by confocal microscopic analysis.

The biofilm samples were live/dead stained for confocal laser scanning microscopy (CLSM) analysis to determine whether mBTL loaded chitosan nanoparticles was capable of killing *S. aureus* cells in biofilms and the results were illustrated in Figure 4. The majority of the *S. aureus* cells were visible to be alive when the biofilm structure was visualized in control (untreated) biofilms (Fig. 5a). On the other hand, biofilm treated with 0.5 mg/ml of mBTL-ChNPs showed an increase in the number of bacteria dead cells throughout biofilm structure (Fig.5b-f). These findings demonstrated that the biofilm treatment with mBTL-ChNPs caused significant cell death within the biofilm.

Preprints (www.preprints.org) | NOT PEER-REVIEWED | Posted: 8 June 2023 doi:10.20944/preprints202306.0628.v1

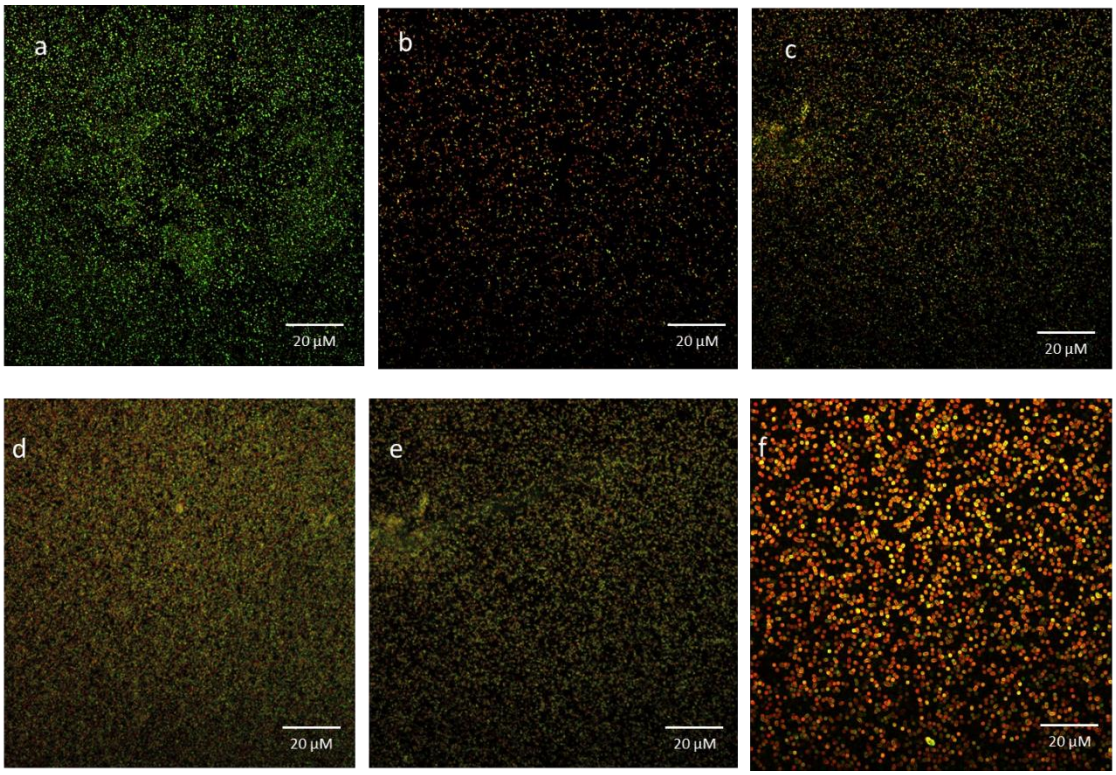

Figure 5. CLSM of Baclight® Live/Dead® (Syto-9 and PI) stained bacterial cells in absence and presence of m-BTL-ChNPs. The Killing impact of m-BTL in comparison the control group is depicted: (a) shows the control group bacterial cells in absence of m-BTL, the green color indicates 98% living cells.; (b-e) bacterial cells treated with m-BTL-ChNPs demonstrated change in cell viability, as evidenced by the appearance of the red/yellow color that indicate dead cells, as well as a change in the morphology of the bacterial cells; (f) Demonstrates that overtime, 92% of the bacterial cells have died.

2.7. SEM Images of m-BTL-ChNPs treated bacterial biofilms.

The morphology of the bacteria in the biofilms formed as a result of exposure to mBTL loaded ChNPs were investigated using SEM and results were demonstrated in Fig.5. As shown in Fig.5a-e, the untreated *S. aureus*, MRSA, *Agr A*, *Agr B*, and *Agr C* mutants showed biofilm formation. When tested isolates were treated with 0.5 mg/ml of m-BTL-ChNPs, marked disruption of the biofilm formation was observed (Fig.6f-j).

Preprints (www.preprints.org) | NOT PEER-REVIEWED | Posted: 8 June 2023 doi:10.20944/preprints202306.0628.v1

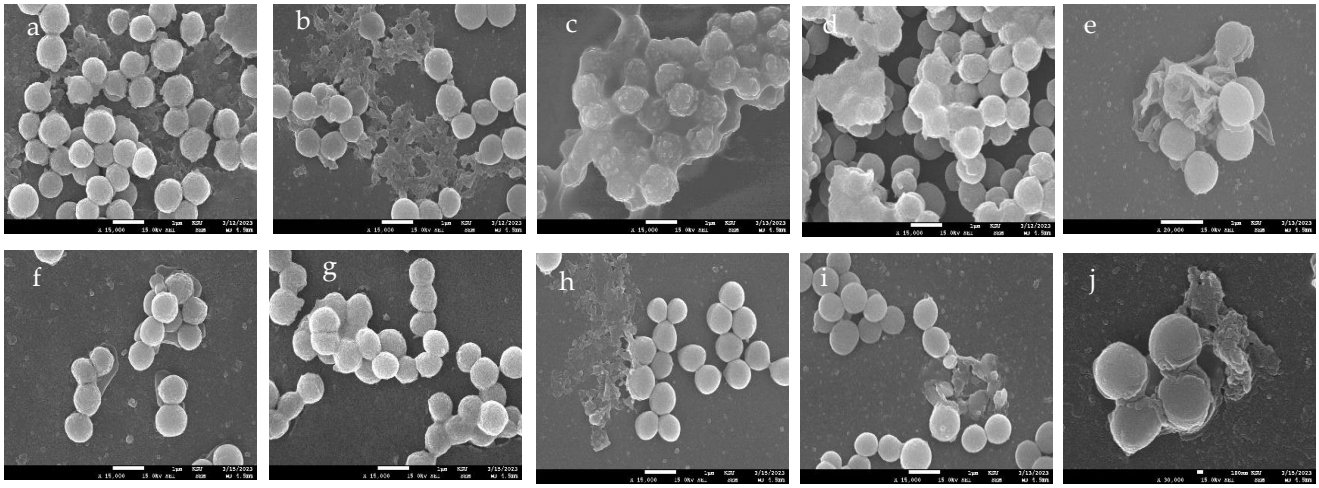

Figure 6. Scanning electron microscopy (SEM) images of a) untreated *S. aureus*, Spherical shaped cells appears in clusters, biofilm is shown as dense extracellular matrix surrounding the cells., b) untreated methicillin resistant *staphylococcus aureus* (*MRSA*), biofilm matrix appears as a dense network of fibres that surround the MRSA cells and connect them to each other., c) Untreated Agr A mutant, shows alteration in cell morphology, the cells appears irregular with a change in surface structure appeared in capsule like formation., d) Untreated *Agr B* mutant, the biofilm looks thick (white shadow) and more surrounding bacterial cells., e) Untreated *Agr C* mutant, biofilm appears more packed over the bacterial cells., f) *S. aureus* treated with loaded mBTL-CNPs, the bacterial cells are separated from each other, and lack a visible extracellular matrix ., g) MRSA treated with loaded mBTL-CNPs, lacks a visible extracellular matrix., h) *Agr A* mutant treated with loaded mBTL-CNPs, shows a disorganization of biofilm separating from the cells., i) *Agr B* mutant treated with loaded mBTL-CNPs, disappearance of the thick biofilm seen in the control (d) with more visibility of bacterial cells., j) *Agr C* mutant treated with loaded mBTL-CNPs, irregular arrangement of biofilm.

2.8. Hemolytic activity of m-BTL-ChNPs on S. aureus strains.

The zone of hemolysis of all bacterial strains treated with mBTL loaded ChNPs were investigated using blood agar and results were demonstrated in Fig.6. As shown in Fig.7a-d, the hemolytic activity of untreated *S. aureus*, MRSA, Agr A, Agr B, and Agr *C* mutants were comparable to bacteria treated with mBTL loaded ChNPs.

Preprints (www.preprints.org) | NOT PEER-REVIEWED | Posted: 8 June 2023 doi:10.20944/preprints202306.0628.v1

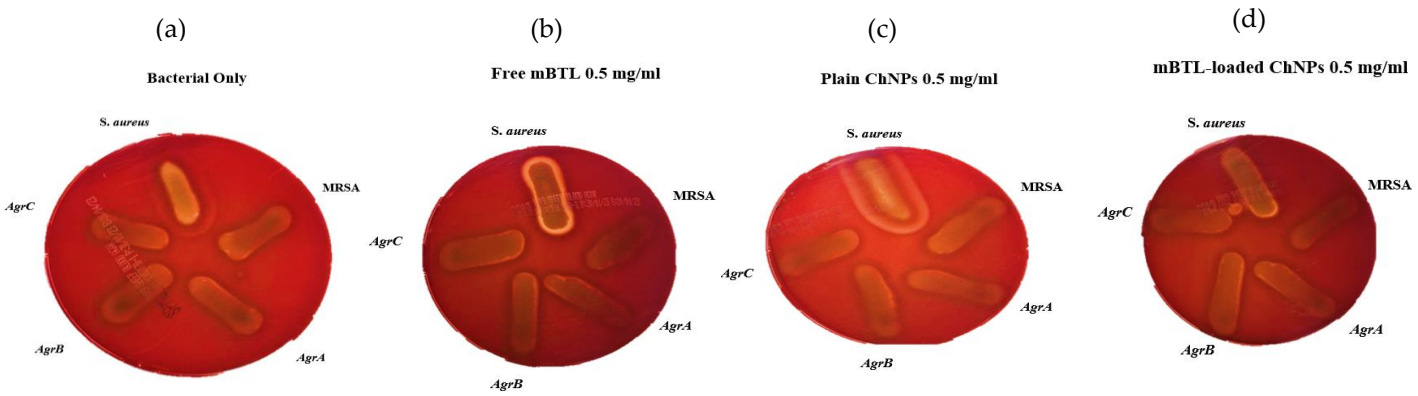

Figure 7. Hemolytic activity of *S. aureus*, MRSA, Agr A mutant, Agr B mutant, and Agr C mutant: (a) Untreated bacterial strains; (b) Treated with free mBTL, c) treated with plain ChNPs and; (d) Treated with mBTL-loaded ChNPs. No significant differences have been shown.

3. Discussion

A MRSA can cause either a skin infection or a blood infection. First is methicillin-resistant Staphylococcus aureus (H-MRSA), which is spread through contact with medical personnel and can result in a variety of unpleasant complications such pneumonia, bacteremia, and surgical site infections. In contrast, community-associated MRSA (C-MRA) causes skin and soft tissue infections in people who have never had contact with a healthcare setting. Despite this, MRSA infections continue to be a leading cause of increased mortality, healthcare expenses, and lengthened hospital stays [14]. Anti-QS molecules such as mBTL, is one of the approaches used for targeting microbial virulence as reported previously. Previous study performed in our lab revealed antimicrobial and antibiofilm activity of mBTL-calcium alginate NPs against different pseudomonal isolates. Therefore, this study aimed to formulate mBTL in CNPs and evaluate their antimicrobial and antibiofilm activity.

In agreements with previous studies [15, 16], plain nanoparticles, and mBTL loaded chitosan nanoparticles were synthesized and showed particle size of 158±1.3 nm and 283.9±13.55 nm, respectively with positive surface charge making these nanoparticles easily up taken by *S. aureus* and other strains due to the negative charge of the organisms.

Microbiological examination and a comparison to free mBTL were performed on mBTL-loaded CNPs. The antagonist activity of the AIP can be obtained by substitutions, truncations or combinations of these modifications for the native AIP. The mBTL is a synthetic analogue *of* Acyl-*HSL, other synthetic analogues have been tested for* quorum sensing inhibition in *S. aureus. these compounds exert their action by* noncompetitive inhibition of the AIP by alteration the activation efficacy of the AIP, they may act as an allosteric inhibitor of AgrC [17, 18].

The selected concentrations of mBTL were 2 mg/ml, 1 mg/ml and 0.5 mg/ml. The concentration (2mg/ml) of mBTL has the greater effect on the different strains of *S. aureus*. Furthermore, the findings of this study revealed that mBTL inhibited bacterial growth of *S. aureus* wild type, *MRSA*, and other QS mutants. Interestingly, this antimicrobial activity was enhanced upon loading of mBTL in ChNPs as observed from the growth curve results. The obtained superiority of loaded mBTL over free mBTL in inhibiting bacterial growth were in agreements with other studies [19].

Biofilms are a type of microbial community that has adapted to living in various habitats, such as on human skin and other medical equipment. They are responsible for two-thirds of all infections and pose a significant risk in medical (and industrial) settings. Microorganisms that form biofilms

 doi:10.20944/preprints202306.0628.v1

are notoriously difficult to treat because they exhibit a form of multidrug resistance called adaptive multidrug resistance [20]. Conventional antibiotics' failure to eradicate biofilms has been traced to several causes. Antibiotic resistance is multifaceted, encompassing biofilm formation, adaptive stress responses, and metabolic inactivation caused by nutrition and gas constraint [21].

Gram-positive bacterial QS systems have peptide autoinducers that are encoded in the genome, allowing the creation of peptides that are specific to each species. The gram-positive opportunistic bacterium *Staphylococcus aureus* is responsible for nosocomial illnesses, such as, sepsis and pneumonia. Methicillin-resistant S. aureus (*MRSA*) and other *S. aureus* strains with resistance to a variety of B -lactam antibiotics are on the rise. Virulence is regulated by the QS system, which is the accessory gene regulator (Agr). The RNAII and RNAIII transcripts are transcribed by the P2 and P3 promoters. In order to regulate the feed forward loop for quorum-sensing autoinducer peptide expression, a transcript encoding the AgrBDCA locus is required. In *S. aureus* the QS systems is required for gene expression, escape from the immunity and establish an infection. The system is encoded by chromosomal locus named the accessory gene regulator (*agr*). The locus consists of two operons produced by P2 and P3 promoters. The P2 have *agrBDCA* and control the RNAII transcript. While the P3 control the RNAIII transcription, which is consider the effector molecule of the *agr* locus. The communication within the cells is managed by AIP, this peptide consists of a thiolactone ring which synthesized by condensation of the carboxyl group in the C-terminus and sulfhydryl group in cysteine. Result in a structure that is necessary for binding of the AIP to its receptor AgrC [22].

The peptide is translated as AgrD precursor, then a transmembrane protein AgrB convert it to a mature AIP and transport the peptide outside the cell. When there are additional bacteria present, the AIP builds up and binds to the AgrC a membrane-bound histidine-kinase, activating the kinas. This activation led to phosphorylation of the agrA which linked to intergenic DNA between P2 and P3, lead to transcription activation. Increases the transcription cause an increase in the intracellular concentrations of RNAIII which is responsible for the translation of the secreted virulence factor. For example, the *hla* which encode the α-toxin and reduce the expression of surface adhesins, such as the protein A and fibronectin-binding protein [23]. Also, the RNAIII stabilizes *mgrA* mRNA and this will increase a global transcriptional regulator called Mgr which serve as intermediate regulator for the *agr* to do its function. The Mgr affect gene involved in virulence, such as autolysis, antibiotic resistance, and biofilm formation [24].

The 4547-residue pro-AIP is synthesized by AgrD, and the 79-residue AIP is then processed and secreted by the AgrB transporter. Through a thiolactone link between the C-terminus and a cysteine residue, the pro-AIP is truncated and cyclized into a five-residue peptide. When there are additional bacteria, the AIP builds up and binds to the Agr C membrane-bound histidine-kinase, activating the QS system. AgrA, the response regulator protein kinase, phosphorylates a conserved histidine and transfers the phosphate group to an aspartate residue. By attaching the upstream of the P2 promotor, AgrA activates the feed-forward the loop and causes the agr operon to be expressed. The hld gene, which codes for the virulence factor -hemolysin, is expressed via the PIII promoter, which is under AgrA's control. On the one hand, RNAIII promotes the expression of -toxin, while on the other, it inhibits the activity of rot factor (a repressor of toxins). Secretion of virulence factors and suppression of factors that control toxin synthesis are both outcomes of this QS regulatory cascade. Additionally, the QS system inhibits biofilm development in the HCD environment while regulating it in the LCD environment. As a result, the biofilm serves as a safe haven for the bacteria to continue multiplying until HCD is attained, after which they can go on to other hosts [25].

Inactive *agr*-system provide an advantage to the *S. aureus* to be better adapt and persistence in the host cell. The *agr*-system has an important role in biofilm development and the *agr*-mutant have a high tendency to form biofilm, cells disseminate from the biofilm showed active *agr*-system. Thus, suppression of the *agr*-system is required for biofilm formation. In this study the mBTL (0.5 mg/ml) encapsulating ChNPs cause a reduction in the biofilm formation of *S. aureus*, *MRSA* by 51.7%, 50% respectively. A higher reduction was observed with mutant strains which have a significant ability for biofilm formation compared with wild-type. The biofilm reduced by; 68%, 63.6% for AgrA, AgrB respectively and 97.3% for AgrC suggesting a potent inhibitory activity for the mBTL- ChNPs [24].

Preprints (www.preprints.org) | NOT PEER-REVIEWED | Posted: 8 June 2023 doi:10.20944/preprints202306.0628.v1

In the current study, mBTL (0.5 mg/ml) encapsulating ChNPs reduced biofilm formation of S. aureus, MRSA, AgrA, and AgrB by 51.7%, 50%, 68% and 63.6%, respectively, and inhibited biofilm development in AgrC by 97.3%. These results were consistent with previous reports in which chrysin loaded ChNPs exhibited marked anti-biofilm activity against S. aureus when compared with untreated bacteria [26]. Other study showed that chitosan-coated iron oxide nanoparticles successfully prevented bacterial colonization and reduced the development of biofilm in S. aureus by 53% [27]. Furthermore, CLSM and SEM were utilized to visualize anti-biofilm activity of mBTL loaded ChNPs towards bacterial isolates tested and the results indicated a decrease in the thickness and density of the biofilm matrix in the presence of NPs.

Chitosan's biodegradability, biocompatibility, and low toxicity have sparked substantial research into its potential uses in a wide variety of sectors. Some of chitosan's many potential applications: as a hydrogel film in the pharmaceutical industry [28], as a flocking agent in water treatment [28], as an elicitor to activate plant defenses [29], as an additive in the food preservation process [30], and as a drug delivery carrier [31].[32-35]. Many reports have also revealed chitosan's broad antibacterial action against bacteria and fungus. The antibacterial action of chitosan, however, is very microorganism-specific [36-38]. Furthermore, chitosan's physicochemical properties are related to the mechanisms of its antibacterial activity. [39,40].

Gram-positive bacterium Staphylococcus aureus is an exceptionally adaptable and flexible pathogen. It is a harmless commensal that can reside on the skin and in the mucous membranes.[41]. However, S. aureus is also one of the top causes of hospital- and community-acquired infections globally due to its ability to grow in the circulation and in numerous tissues, causing significant disease [42, 43]. It can trigger anything from a simple skin infection to more serious systemic infections that can even be fatal, such pneumonia, osteomyelitis, and endocarditis. S. aureus infections can recur in 8-33% of cases, leading to significant human morbidity and mortality [30].

O'Loughlin CT, et al, showed that mBTL's effects extended beyond those of an anti-infective agent; it also reduced the development of biofilms and the clogging of microfluidic devices. However, it was suggested that the employing of anti-quorum-sensing molecules might prevent the failure of systems that are susceptible to fouling by biofilms.[4]. As a result, these molecules may find applications in fields as diverse as industry and the field of medicine. Here, we employed liquid administration of the inhibitor; ultimately, we hope to include mBTL-like molecules into the materials used to manufacture such gadgets, making those goods inherently resistant to biofilms. Together, our results on mBTL provide strong evidence for the efficacy of quorum-sensing modulators in reducing pathogens with quorum-sensing-controlled phenotypes.

Eltayb EK, et al., also agreed with our results in the effectiveness of loaded-mBTL in decreasing minimum inhibitory concentration of mBTL for different Pseudomonal isolates tested [13].

To our knowledge limited number of studies were conducted to investigate the effect of loaded-mBTL on different bacterial strains, and most of these studies have been conducted on Pseudomonas aeruginosa; this makes our study pioneering in investigating mBTL and loaded-mBTL effect on different Staphylococcus strains. The promising results of loaded-mBTL gives hope for rising new generations of drug that can treat a group of resistant bacteria and decrease the consumption of antibiotics.

4. Materials and Methods

4.1. Bacterial strains, chemicals, and growth conditions

Strains of *Staphylococcus aureus*, MRSA, and different QS mutants as described in Table 1, were grown in tryptic soy broth (TSB) and tryptic soy Agar (TSA) supplemented with is erythromycin and incubated at 37 ºC for 18-24 hr [8].

Preprints (www.preprints.org) | NOT PEER-REVIEWED | Posted: 8 June 2023 doi:10.20944/preprints202306.0628.v1

Table 1. Description of Staphylococcus aureus strains in this study.

Strain Name	Abbreviation	Description
Staphylococcus aureus	*S. aureus*	wild type
Methicillin-Resistance *Staphylococcus aureus*	MRSA	Methicillin-Resistance *Staphylococcus aureus*
NE1532	AgrA	4 P16 agrA accessory gene regulator protein A SAUSA300_1992
NE95	AgrB	1 O21 agrB accessory gene regulator protein B SAUSA300_1989
NE873	AgrC	3 B17 agrC accessory gene regulator protein C SAUSA300_1991

4.2. Preparation of chitosan nanoparticles (ChNPs) and mBTL loading

ChNPs were prepared using the ionic gelation method by dissolving 10 ml of 1% v/v acetic acid in 100 ml of deionized water, and then 100 mg of chitosan was added and magnetically stirred for 2-3 hr until it was completely dissolved. The nanoparticles could be affected by the acidic media; accordingly, the solution pH was adjusted using sodium hydroxide (NaOH) to pH of 4.7. mBTL 4% was dissolved in 1200 µl DMSO and 1000 µl of tween 20, the resulted mixture was then added to the prepared chitosan solution. To 10 mL of chitosan solution containing the drug, DMSO, and tween 20, 4 mL of 0.01 % w/v TPP solution was added. This mixture was then continuously magnetically stirred at 500 rpm for 30 min. The nanoparticles were formed. The nanoparticle solution was then centrifuged twice at 14000 rpm for 30 min using a cooling centrifuge. The retrieved nanoparticles were then suspended in deionized water. Finally, the ChNPs were reconstituted in deionized water and stored at 4°C for further characterization.

4.3. Physicochemical analysis of mBTL-loaded ChNPs

The mean particle size, polydispersity index and zeta potential of mBTL-ChNPs was measured at 25 °C using the Zeta sizer Nano ZS (Malvern Instruments, Malvern, UK). The nanoparticle suspension was diluted 5 times with deionized water. All measurements were performed in triplicate.

4.4. Determination of mBTL-loaded ChNPs encapsulation efficiency (EE %)

The encapsulation efficiency of mBTL-ChNPs was indirectly determined by measuring the concentration of free mBTL in the aqueous phase. The encapsulation efficiency was estimated using the following equation:

$$\textbf{\%Entrapment Efficiency} = \frac{\text{total amount of drug loaded} - \text{free drug in supernatant}}{\text{total amount of drug loaded}} \; x\,100 \qquad (1)$$

4.5. In vitro release of mBTL-ChNPs

The release profiles of mBTL-ChNPs were evaluated by means of the dialysis method using cellulose dialysis tube sealed at both ends. The membrane was soaked in a release medium overnight before use. One ml of mBTL-ChNPs was placed into dialysis bags, which were then transferred into beakers containing 30 mL of the phosphate buffer pH 7.4. At predetermined time intervals 0.5, 1, 2, 4, 5, 6, 7, 8 and 24, 48 hours, 3 mL of the release medium was withdrawn and instantly replaced by an equal amount of fresh release medium to maintain a sink condition. The amount of released mBTL

Preprints (www.preprints.org) | NOT PEER-REVIEWED | Posted: 8 June 2023 doi:10.20944/preprints202306.0628.v1

was determined by measuring the absorbance at 280 nm. The release profile of mBTL was obtained by plotting the cumulative percentage release of the drug versus time.

4.6. Growth Curve Construction

All bacterial strains were grown in 5 ml TS broth with the selected antibiotic marker Erythromycin except for the fourth wild type of strain, then incubated at 37 ºC with continuous overnight shaking at 200 rpm. 200 µl of bacterial broth with optical density of 0.4-0.6 McFarland was added to 96 well plates. All tests were performed in triplicate and controls of media only and untreated bacteria, then the 96 well plates were placed in BioscreenC reader and optical density of bacterial growth was recorded at 600 nm for 24 hr.

4.7. MIC measurements

According to the CLSI guidelines, the MBC is defined as the first dilution that results in three or fewer colonies after 24 hours of incubation at 37 °C.The double-dilution method [9, 11] is the standard method for determining minimal inhibitory concentrations (MICs). The minimal inhibitory concentrations were determined by measuring the concentration of the formula at which no visible growth occurred. The minimal bactericidal concentration (MBC) was also recorded as the lowest concentration of the compound at which no colonies formed after plating the dilutions around the MIC or growing them in fresh TSB media. For all strains MBCs were determined by inoculation of 10 µl from each well that did not show visible bacterial growth on TS plates. After 24 h of incubation at 37 °C, the first dilution yielded three colonies or fewer was scored as the MBC, as described by the CLSI.

4.8. Hemolytic Activity Analysis

For hemolytic activity an overnight culture of all strains was standardized to $OD_{600}$of 0.5 and 1:50 diluted in 10 mL TSB with or without antibiotic and tested formula. Strains were streaked on blood agar plates, incubated overnight at 37°C for 24 and 48 hr. The hemolytic activity was observed on plates as transparency around the colonies [9].

4.9. Biofilm Assay

Modifications were made to the method previously described for detecting biofilms [10]. Strains were cultivated at 37 °C for 24 hr in TSB broth, diluted to 107 cfu/ml in TSB media, and dispensed in 96-well microliter plates (Thomas science). Then, 100 µL of each antibiotic and compounds at 1 mg/mL FC were added to each well. Biofilm inhibition was evaluated by inoculating 15-well plates with each strain (100 µL of bacterial strain was added to each well) and incubating the plates at 37°C for 24 hr. After removing the cell suspension, the plates were washed twice with a 0.9% NaCl solution and air dried at room temperature for 1 hr. After 15 min, the wells were stained with 150 µl of crystal violet solution (CV; Prolab Diagnostics). Following staining, CV was removed, and 0.9 % NaCl solution was used to wash the wells three times. The attached CV was dissolved in 200 µl of ethanol-acetone (80:20 v/v). Finally, a microplate reader was used to measure the CV absorbance at 595 nm (BioTek). All experiments were carried out in triplicate for three independent times.

4.10. Confocal Microscopy

All isolates were cultured in Tryptic soy agar (TS) or TS agar supplemented with 10 mg/mL erythromycin at 37 °C for 18 hr. The culture media were purchased from Oxoid (Basingstoke, Hampshire, UK). 5 samples were treated with 0.5 mg/ml free mBTL. The effect of m-BTL on bacterial cell viability was determined by confocal laser scanning microscope, CLSM, (Leica TCS SP5, UK) with a Live/Dead® BacLight™ viability kit consisting of a universal stain SYTO 9 and propidium iodide (PI). Cells images were acquired using the Leica Application Suite Advanced Fluorescence software 5 (Leica, UK), with an optical magnification of 40× using an oil-immersion objective lens. Images were sized to 1024 × 1024 pixels and recorded by scanning lasers over an area of 25 × 25 µm. An argon-based laser was employed for excitation at 488 nm, and HeNe laser for excitation at 543 nm. The

 doi:10.20944/preprints202306.0628.v1

emission was set at 528 nm for SYTO 9 and 645 nm for PI. Via sequential scanning, the images were obtained and processed in Image J software.

4.11. Scanning Electron Microscopy (SEM)

In order to visualize biofilm formation, bacteria were grown overnight in LB at 37 °C. Next day the cultures were diluted in LB to 10^7cfu/ml. Polyvinyl (Fisher Scientific) coverslips were placed in each well of a Thomas 6-well plate before being filled with 2 ml of LB medium and 2 ml of diluted culture. Biofilms were then formed on the coverslips at 37 °C for 24 hr. Biofilm samples were fixed with 3% glutaraldehyde in phosphate buffer pH 7.2 for 24 h. after three washes with phosphate buffer, samples were postfixed for 1 h with 1% osmium tetroxide (in H_2O), and then were applied in to an ethanol dehydration series of 50, 60, 70, 80, 90, and 2 × 100% (v/v) ethanol, for 5 min at each concentration [12]. All samples were then dried for 1 day and sputter-coated with a palladium-gold thin film. SEM/EDS imaging of the biofilm was performed in a high-vacuum mode at 20 kV using an FEI Quanta 400FEG ESEM/EDAX Genesis X4M (FEI Company, USA).The produced biofilm was viewed with a SEM/EDS system (FEI Quanta 400FEG ESEM/EDAX Genesis X4M, FEI Company, USA) in a high-vacuum mode at 20 kV.

5. Conclusions

Inhibition of quorum sensing is widely recognized as an effective anti-virulence approach. The developed mBTL loaded chitosan nanoparticles showed enhanced antibacterial activity against all tested staphylococcal strains relative to mBTL alone. Furthermore, prepared NPs reduced biofilm formation as revealed by crystal violet staining, CLSM and SEM. Findings of this study suggested a potential future therapeutic use of synthesized mBTL-ChNPs in the treatment of S. aureus infection and prevention of biofilm formation.

Author Contributions: FSA, FYA and RTA: Conceptualization, design of study, methodology, acquisition of data, validation, supervision Resources, visualization and writing final draft preparation. EKE, BMA and ASA: Acquisition of data, analysis of data, visualization, interpretation of data and writing first draft preparation. HA chemical synthesis and analysis of mBTL and interpretation of all chemical analysis. EE nanoparticles formulation and analysis. SH and NAA interpretation of data and writing first draft. TAA validation, Resources, visualization and writing final draft preparation. All authors have read and agreed to the published version of the manuscript.

Funding: This research project was supported by the Researchers Supporting Project number (RSP2023340), King Saud University, Riyadh, Saudi Arabia.

Institutional Review Board Statement: Not applicable.

Informed Consent Statement: Not applicable.

Data Availability Statement: The data presented in this study are available on request from the corresponding author.

Acknowledgments: The authors extend their sincere appreciation to the Researchers Supporting Project number (RSP2023340), King Saud University, Riyadh, Saudi Arabia.

Conflicts of Interest: The authors declare no conflict of interest.

 doi:10.20944/preprints202306.0628.v1

References

1. Al Bshabshe, A., Joseph, M., Awad El-Gied, A., Fadul, A., Chandramoorthy, H. andHamid M. Clinical Relevance and Antimicrobial Profiling of Methicillin-ResistantStaphylococcus aureus (MRSA) on Routine Antibiotics and Ethanol Extract of Mango Kernel. Biomed Res Int. Published online 2020:1-8.
2. Nielsen, A., Månsson, M., Bojer, M., Gram, L., Larsen, T., Novick, R., Frees, D., Frøkiær, H. and Ingmer H. Solonamide B Inhibits Quorum Sensing and ReducesStaphylococcus aureus Mediated Killing of Human Neutrophils. PLoSONE,. 2014;9(1).
3. Choudhary KS, Mih N, Monk J, Kavvas E, Yurkovich JT, Sakoulas G PB. TheStaphylococcus aureus Two-Component System AgrAC Displays Four DistinctGenomic Arrangements That Delineate Genomic Virulence Factor Signatures. Front Microbiol. 25;9:(1082).
4. O'Loughlin CT, Miller LC, Siryaporn A, et al. A quorum-sensing inhibitor blocksPseudomonas aeruginosa virulence and biofilm formation. Proceedings of theNational Academy of Sciences. 2013: 16981-96. *Home - PMC - NCBI* (no date) *National Center for Biotechnology Information*. U.S. National Library of Medicine. Available at: https://www.ncbi.nlm.nih.gov/pmc/ (Accessed: January 4, 2023).
5. Alshamsan, A., Aleanizy, F.S., Badran, M., Alqahtani, F.Y., Alfassam, H., Almalik, A. and Alosaimy, S., 2019. Exploring anti-MRSA activity of chitosan-coated liposomal dicloxacillin. *Journal of microbiological methods*, *156*, pp.23-28.
6. Reddy, C.A., Beveridge, T.J., Breznak, J.A. and Marzluf, G. eds., 2007. Methods forgeneral and molecular microbiology. American Society for Microbiology Press.
7. Burnside, K., Lembo, A., de Los Reyes, M., Iliuk, A., BinhTran, N.T., Connelly, J.E.,Lin, W.J., Schmidt, B.Z., Richardson, A.R., Fang, F.C. and Tao, W.A., 2010.Regulation of hemolysin expression and virulence of Staphylococcus aureus by a serine/threonine kinase and phosphatase. PloS one, 5(6), p.e11071.
8. Zhao D, Yu S, Sun B, Gao S, Guo S, Zhao K. Biomedical applications of chitosan and its derivative nanoparticles [Internet]. Polymers. U.S. National Library of Medicine; 2018 [cited 2022Nov22]. Available from: https://www.ncbi.nlm.nih.gov/pmc/articles/PMC6415442/
9. Hoang NH, Le Thanh T, Sangpueak R, Treekoon J, Saengchan C, Thepbandit W, et al. Chitosan nanoparticles-based Ionic gelation method: A promising candidate for Plant Disease Management [Internet]. Polymers. U.S. National Library of Medicine; 2022 [cited 2022Nov22]. Available from: https://www.ncbi.nlm.nih.gov/pmc/articles/PMC8876194/
10. Owuama, C.I., 2017. Determination of minimum inhibitory concentration (MIC) and minimum bactericidal concentration (MBC) using a novel dilution tube method. African journal of microbiology research, 11(23), pp.977-980.
11. Marrie, T. and Costerton, J.W., 1984. Scanning and transmission electron microscopy of in situ bacterial colonization of intravenous and intraarterial catheters. Journal of Clinical Microbiology, 19(5), pp.687-693.
12. Eltayb EK, Alqahtani FY, Alkahtani HM, Alsarra IA, Alfaraj R, Aleanizy FS. Attenuation of Pseudomonas aeruginosa Quorum Sensing Virulence of Biofilm and Pyocyanin by mBTL-Loaded Calcium Alginate Nanoparticles. Polymers. 2022 Sep 2;14(17):3655.
13. Khan, S.; Tondervik, A.; Sletta, H.; Klinkenberg, G.; Emanuel, C.; Onsoyen, E.; Myrvold, R.; Howe, R.A.; Walsh, T.R.; Hill, K.E.; et al. Overcoming drug resistance with alginate oligosaccharides able to potentiate the action of selected antibiotics. Antimicrob. Agents Chemother. 2012, 56, 5134–5141.
14. Herdiana Y, Wathoni N, Shamsuddin S, Muchtaridi M. Drug release study of the Chitosan-based nanoparticles. Heliyon. 2022;8(1).
15. Shi, S.F.; Jia, J.F.; Guo, X.K.; Zhao, Y.P.; Chen, D.S.; Guo, Y.Y.; Zhang, X.L. Reduced Staphylococcus aureus biofilm formation in the presence of chitosan-coated iron oxide nanoparticles. Int. J. NanoMed. 2016, 11, 6499–6506. [CrossRef]
16. Fadilah Sfouq Aleanizy, Fulwah Yahya Alqahtani, Gamal Shazly, Rihaf Alfaraj, Ibrahim Alsarra, Aws Alshamsan, Hosam Gareeb Abdulhady, Measurement and evaluation of the effects of pH gradients on the antimicrobial and antivirulence activities of chitosan nanoparticles in Pseudomonas aeruginosa,Saudi Pharmaceutical Journal, Volume 26, Issue 1, 2018,Pages 79-83,
17. Suligoy CM, Lattar SM, Noto Llana M, González CD, Alvarez LP, Robinson DA, Gómez MI, Buzzola FR and Sordelli (2018) Mutation of Agr Is Associated with the Adaptation of *Staphylococcus*

 doi:10.20944/preprints202306.0628.v1

aureus to the Host during Chronic Osteomyelitis. Front. Cell. Infect. Microbiol. 8:18. doi: 10.3389/fcimb.2018.00018

18. Murray EJ, Crowley RC, Truman A, Clarke SR, Cottam JA, Jadhav GP, Steele VR, O'Shea P, Lindholm C, Cockayne A, Chhabra SR, Chan WC, Williams P(2014) Targeting Staphylococcus aureus quorum sensing with nonpeptidic small molecule inhibitors. J Med Chem. 27;57(6):2813-9. doi: 10.1021/jm500215s
19. Mandal SM, Ghosh AK, Pati BR. Dissemination of antibiotic resistance in methicillin-resistant Staphylococcus aureus and vancomycin-resistant S aureus strains isolated from hospital effluents. American journal of infection control. 2015 Dec 1;43(12): e87-8.
20. Novick RP. Autoinduction and signal transduction in the regulation of staphylococcal virulence. Molecular microbiology. 2003 Jun;48(6):1429-49.
21. Boles BR, Horswill AR. Agr-mediated dispersal of Staphylococcus aureus biofilms. PLoS Pathog. 2008 Apr 25;4(4):e1000052. doi: 10.1371/journal.ppat.1000052.
22. Yarwood JM, Bartels DJ, Volper EM, Greenberg EP. Quorum sensing in Staphylococcus aureus biofilms. J Bacteriol. 2004 Mar;186(6):1838-50. doi: 10.1128/JB.186.6.1838-1850.2004. PMID: 14996815.
23. Gupta RK, Luong TT, Lee CY. RNAIII of the Staphylococcus aureus agr system activates global regulator MgrA by stabilizing mRNA. Proc Natl Acad Sci U S A. 2015 Nov 10;112(45):14036-41. doi: 10.1073/pnas.1509251112.
24. Krismer B, Peschel A. Does Staphylococcus aureus nasal colonization involve biofilm formation? Future microbiology.6(5):489-93.
25. Mandal SM, Ghosh AK, Pati BR. Dissemination of antibiotic resistance in methicillin-resistant Staphylococcus aureus and vancomycin-resistant S aureus strains isolated from hospital effluents. American journal of infection control. 2015 Dec 1;43(12): e87-8.
26. Messias de Souza, Gabrielle & Gervasoni, Leticia & Rosa, Rafael & Iacia, Maria & Nai, Gisele & Pereira, Valeria & Winkelströter, Lizziane. (2022). Quercetin-loaded chitosan nanoparticles as an alternative for controlling bacterial adhesion to urethral catheter. International Journal of Urology. 29. 10.1111/iju.14958.
27. Siddhardha, B.; Pandey, U.; Kaviyarasu, K.; Pala, R.; Syed, A.; Bahkali, A.H.; Elgorban, A.M. Chrysin-Loaded Chitosan Nanoparticles Potentiates Antibiofilm Activity against Staphylococcus aureus. Pathogens 2020, 9, 115. https://doi.org/10.3390/pathogens9020115
28. Abebe, L.S.; Chen, X.; Sobsey, M.D. Chitosan coagulation to improve microbial and turbidity removal by ceramic water filtration for household drinking water treatment. Int. J. Environ. Res. Public Health 2016, 13, 269.
29. Herdiana Y, Wathoni N, Shamsuddin S, Muchtaridi M. Drug release study of the Chitosan-based nanoparticles. Heliyon. 2022;8(1).
30. Sharifi-Rad J, Quispe C, Butnariu M, Rotariu LS, Sytar O, Sestito S, et al. Chitosan nanoparticlesas a promising tool in nanomedicine with particular emphasis on oncologicaltreatment. CancerCell International. 2021;21
31. Diekema, D. J., et al. "Continued Emergence of USA300 Methicillin-Resistant Staphylococcus aureus in the United States: Results from a Nationwide Surveillance Study." Infect. Control Hosp. Epidemiol. 35 (2014): 285- 292. PubMed: 24521595.
32. Cota-Arriola, O.; Cortez-Rocha, M.O.; Burgos-Hernandez, A.; Ezquerra-Brauer, J.M.; Plascencia-Jatomea, M. Controlled release matrices and micro/nanoparticles of chitosan with antimicrobial potential: Development of new strategies for microbial control in agriculture. J. Sci. Food Agric. 2013, 93, 1525–1536.
33. Agullo, E.; Rodriguez, M.S.; Ramos, V.; Albertengo, L. Present and future role of chitin and chitosan in food. Macromol. Biosci. 2003, 3, 521–530
34. Felt, O.; Buri, P.; Gurny, R. Chitosan: A unique polysaccharide for drug delivery. Drug Dev. Ind. Pharm. 1998, 24, 979–993
35. Alvarez Echazu, M.I.; Olivetti, C.E.; Anesini, C.; Perez, C.J.; Alvarez, G.S.; Desimone, M.F. Development and evaluation of thymol-chitosan hydrogels with antimicrobial-antioxidant activity for oral local delivery. Mater. Sci. Eng. C Mater. Biol. Appl. 2017, 81, 588–596.
36. Sharma, P.K.; Halder, M.; Srivastava, U.; Singh, Y. Antibacterial PEG-chitosan hydrogels for controlled antibiotic/protein delivery. ACS Appl. Bio Mater. 2019, 2, 5313–5322.
37. Chen, C.P.; Hsieh, C.M.; Tsai, T.; Yang, J.C.; Chen, C.T. Optimization and evaluation of a chitosan/hydroxypropyl methylcellulose hydrogel containing toluidine blue O for antimicrobial photodynamic inactivation. Int. J. Mol. Sci. 2015, 16, 20859–20872

 doi:10.20944/preprints202306.0628.v1

38. Li, B.; Shan, C.L.; Ge, M.Y.; Wang, L.; Fang, Y.; Wang, Y.L.; Xie, G.L.; Sun, G.C. Antibacterial mechanism of chitosan and its applications in protection of plant from bacterial disease. Asian J. Chem. 2013, 25, 10033–10036.
Varlamov, V.P.; Mysyakina, I.S. Chitosan in biology, microbiology, medicine, and agriculture. Microbiology 2018, 87, 712–715
39. Rabea, E.I.; Badawy, M.E.T.; Stevens, C.V.; Smagghe, G.; Steurbaut, W. Chitosan as antimicrobial agent: Applications and mode of action. Biomacromolecules 2003, 4, 1457–1465
Younes, I.; Rinaudo, M. Chitin and chitosan preparation from marine sources. Structure, properties and applications. Mar. Drugs 2015, 13, 1133–1174.
40. Xing, K.; Zhu, X.; Peng, X.; Qin, S. Chitosan antimicrobial and eliciting properties for pest control in agriculture: A review. Agron. Sustain. Dev. 2015, 35, 569–588
41. Bamm VV, Ko JT, Mainprize IL, Sanderson VP, Wills MK. Lyme disease frontiers: Reconciling borrelia biology and clinical conundrums. Pathogens. 2019 Dec 16;8(4):299.
42. Aggarwal S, Mahajan P, Gupta P, Yadav A, Dhawan G, Dhawan U, Yadav AK. The bacterial communication system and its interference as an antivirulence strategy. InBacterial Survival in the Hostile Environment 2023 Jan 1 (pp. 163-191). Academic Press.
43. Novick RP. Autoinduction and signal transduction in the regulation of staphylococcal virulence. Molecular microbiology. 2003 Jun;48(6):1429-49.